Copyright © 2007 by ABCM

FROM NANO TO MACROMECHANICS: A MOLECULAR MECHANICS ANALYSIS OF SINGLE-WALLED CARBON NANOTUBES

Antonio F.Avila, aavila@netuno.lcc.ufmg.br
Gulherme S.R. Lacerda, guirachid@yahoo.com.br
Universidade Federal de Minas Gerais, Department of Mechanical Engineering, Mechanics of Composites and Nano-structured Materials Laboratory, 6627 Antonio Carlos Avenue, Belo Horizonte, MG 31270-901, Brazil

Abstract. *Carbon nanotubes are considered the stiffest material known. In addition to high stiffness, around 1.0 TPa, this class of new materials, with diameter around 1.0 nm and length of 1.0 μm, exhibts remarkable electrical and thermal proprieties. With such great properties, this class of materials is the natural choice for high performance materials. The problem, however, rises when the experimental data are compared against each other. The large variability of experimental data lead to development of a new set of numerical simulations called molecular mechanics. Such numerical technique results is a "simbiotic" association of molecular dynamics and solid mechanics, in special the finite element method. This papers deals with a molecular mechanics simulation of single-walled carbon nanotubes. Three main carbon nanotubes configurations were simulated, i.e armchair, zigzag and chiral. From te concept of representative unit cell, and applying the molecular mechanics principles the carbon nanotubes stiffeness were predicted. It was showed that not only the carbon nanotube configuration has influence on stiffness but radius is also a important variable. By varying the radius the Young's modulus changed from 0.95 TPa to 1.03 TPa. The numerical simulations were in good agreement with those presented in literature.*

Keywords*: Carbon Nanotubes, Molecular Mechanics, Stiffness, Finite Element Method.*

1. INTRODUCTION

According to Saito et al. (2005), carbon nanotube is a honeycomb lattice rolled into a cylinder. What do this class of material special are its dimensions and consequently its mechanical and electrical properties. In general, a carbon nanotube diameter is of nanometer size and its length can be more than 1μm. As mentioned by Saito and his colleagues, nanotube diameter is much smaller than most advanced semiconductors devices developed so far. Moreover, consistent with Kalamkarov et al. (2006), carbon nanotubes (CNT) are the stiffest known materials along with a predicted strength of about 100 times that of steel at only one-sixth of the weight. With regard to their thermal properties, carbon nanotubes are thermally stable up to 2800 C (in vacuum), exhibit a thermal conductivity about twice as high as diamond, and may exhibit a capacity to carry electric current a thousand times better than copper wires. With such promising properties, CNT are natural candidates for reinforcement of advanced composites. Nevertheless, variability form experimental data obtained from CNT is a problem.

As stated by Natsuki et al. (2004), experimental methods for measuring the mechanical properties of CNTs are mainly based on the techniques of transmission electron microscopy (TEM) and atomic force microscopy (AFM). They described the results obtained by Treacy et al. for multi-walled carbon nanotubes (MWNT). According to them, by measuring thermal vibration using TEM, Treacy et al obtained a Young modulus of 1.8±0.9TPa. Natsuki et al. (2004) also reported a slightly lower value of 1.28±0.59 TPa with little dependence of nanotube diameter obtained by Wong et al. using the AFM tip to bend anchored MWNTs. A set of experiments performed by Yu et al. (2000) in MWNT lead to data ranging from 11 to 63 GPa and 0.27 to 0.95 TPa to tensile strength and Young's modulus, respectively.

The results obtained for single-walled carbon nanotubes (SWNTs) follow the same pattern. Krishnan et al. (1998) have reported a study on single-walled carbon nanotubes (SWNT) using the TEM technique. The SWNT had a diameter range of 1.0–1.5 nm, and the elastic modulus was measured to be the mean value of 1.30±0.4 TPa. Yu et al. (2000) have also obtained the mechanical responses of SWNT bundles under tensile loading. The values of elastic modulus ranged from 0.32 to 1.47 TPa with a mean value of 1.02 TPa, and a tensile strength from 13 to 53 GPa. Lourie and Wagner (1998) obtained the axial Young's modulus for a series of temperatures by micro-Raman spectroscopy from measurements of cooling-induced compressive deformation of nanotubes embedded in an epoxy matrix. At low temperature, ≈ 80 K, Lourie and Wagner (1998) got a 3.0 TPa axial Young's modulus for SWNT with an average radius of 0.7 nm, and 2.4 TPa for MWNTs with an average radius of 5–10nm. Xiao et al. (2005), however, reported for SWNT the tensile modulus ranged from 0.27 to 3.6 TPa, while the ultimate strength varied from 11 to 200 GPa. With such variability on these results, Xiao et al (2005) concluded that CNT, single or multi-walled, elastic properties are highly dependent on its structure.

Due to the difficulties in experimental characterization of nanotubes, computer simulation has been regarded as a powerful tool for modeling the properties of nanotubes. The fundamental relations governing the geometry of CNT were described by Dresselhaus et al (1995). They were able to explain the mathematical expression that relates the graphene sheet geometry in a honeycomb-like design and the carbon nanotubes three main configurations, i.e. chiral, zigzag and armchair. By doing it, they opened the possibility to CNT computer simulations. For Xiao et al (2005), the

large majority of numerical and analytical approaches can be classified into one of two categories: the "bottom up" approach based on quantum/molecular mechanics including the classical molecular dynamics (MD), and the "top down" based on continuum mechanics. A third category, however, can be established; it is called the multi-scale methods, where the continuum mechanics models are coupled to MD expressions. Wang et al. (2003) reported that MD formulations were probably the most popular method currently employed for nano-scale analysis, due to its availability of accurate interatomic potentials for a range of materials. However, a critical issue on MD simulations remains, i.e. temperature. The temperature induced high frequency molecular thermal vibration, on scale of 10^{15} Hz, makes difficult to estimate strains, even worst, limit the deformation calculations to nano-seconds. In addition to this problem,

Liu et al. (2006) mentioned that in most applications nanoscale materials are used in association to other components that are larger, and have different response times, thus operating at different time and length scales. Furthermore, single scale methods such as *ab initio* quantum mechanical methods or molecular dynamics (MD) will have difficulty in analyzing such hybrid structures due to the limitations in terms of the time and length scales that each method is confined to. Yet, the length and time scales that can be probed using MD are still fairly limited. For the study of nanoscale mechanics and materials, Liu et al. (2006) suggested model up to a scale of several microns, consisting of billions of atoms, which is too large for MD simulations to-date. Hence, there is a need to develop multi-scale approaches for this class of problems.

Li and Chou (2006) defined the multi-scale modeling technique as a combination of the atomistic molecular structural mechanics approach (Li and Chou, 2003) and the continuum finite element method (Zienkiewicz and Taylor, 1989). This approach was also implemented by Meo and Rossi (2006), where the elements selected were both non-linear elastic springs and linear elastic torsional spring. As mentioned by them, the non-linear elastic spring element was applied due to the lack of information about the sectional properties of carbon-carbon bond. Furthermore, the torsional spring element was used to overcome the problems with bond angles bending. They were able to simulate the three main SWNT configurations, i.e. armchair, zigzag and chiral, and graphene sheets. Furthermore, the geometric description of SWNT of their model was based on Cartesian equations proposed by Koloczek et al. (2001). Such approach saved considerable computational efforts during the mesh generation. Their predictions for the grapheme sheets Young's modulus were in good agreement with the ones published in literature, i.e. ≈1.03 TPa. After simulating several SWNT configurations, Meo and Rossi (2006) found out that their predictions were in good agreement with several authors. Although the results provided by Meo and Rossi (2006) were in good agreement with several papers published in literature, their model was limited to uniaxial tensile problems.

To overcome such problem Sun and Zhao (2005) proposed a model based on molecular-mechanics and finite element method. Sun and Zhao (2005) made usage of two types of elements. The first one was a chemical bond element which represented the intra-molecular potential energy of stretching, bending and torsion energies. This element was based on a two-node elastic rod element with an elastic joint in each end. The second element was a Lennard-Jones element which stood for the inter-molecular potential energy. In this case, a spring element with non-linear stiffness derived from the Lennard-Jones energy was applied. Sun and Zhao (2005) went further, by modifying the Morse potential function they were able to modeling the C-C chemical bond breakage. In sum, they were up of modeling stiffness and strength simultaneously. However, the data obtained, 0.4 TPa for stiffness and between 77-101 GPa for strength, were below than the usual results published in literature. A possible explanation for such behavior can be the excess of compliance introduced during stiffness matrix derivation. This hypothesis is corroborated by Pantano et al. (2004) that related the bending stiffness with the mean radius of the tube and its total wall thickness. Note that for Sun and Zhao (2005) the tensile stiffness was practically constant with the increase on nanotube diameter.

The work developed by Huang et al. (2006) gave a step forward by introducing the total energy of the system expressed as a function of the location of the atomic nucleons. The same analogy between stretching and bending elements and the atoms bond were also employed. Furthermore, they introduced a third analogy called inversion. By considering only stretching and bending, their results were similar to Sun and Zhao (2005), but with the introduction of inversion the results converged to a 1.059 TPa value. Tserpes and Papanikos (2005) employed beam elements in a three-dimensional (3D) space where stretching, bending, out-of-plane torsion and dihedral angle torsion were considered. Such model brought about results with good agreement with the literature with minimal computational efforts.

In this paper, the concept of molecular structural mechanics described Li and Chou (2003) associated to the three-dimensional finite element model introduced by Tserpes and Papanikos (2005) is employed to predict the SWNT stiffness. Numerical simulations considering the main configurations, i.e. armchair, zigzag and chiral, are performed. A parametric study on wall thickness, diameter and chirality's effects on stiffness is also objective of this paper.

2. MOLECULAR MECHANICS

Dresselhaus et al. (1995) described SWNT in terms of the tube diameter (d) and its chiral angle (θ). The chiral vector (C_h) was defined in terms of the graphene sheet lattice translation integer indices (n,m) and the unit vectors (a_1,a_2) as follows:

$$\vec{C}_h = n\vec{a}_1 + m\vec{a}_2 \tag{1}$$

where the unit vectors in (x,y) coordinates are defined as:

$$\vec{a}_1 = \left(\frac{\sqrt{3}}{2}, \frac{1}{2}\right)a \qquad \vec{a}_2 = \left(\frac{\sqrt{3}}{2}, -\frac{1}{2}\right)a \tag{2}$$

the length of the unit vector *a* is equals to 2.46 angstroms, or 1.73 times the carbon-carbon distance, i.e. 1.421 angstroms. The nanotube circumference (*p*) was defined by:

$$p = \left|C_h\right| = a\sqrt{n^2 + m^2 + nm} \tag{3}$$

from simple geometry, it is possible to obtain the nanotube diameter (*d*), as:

$$d = \frac{p}{\pi} = \frac{\sqrt{n^2 + m^2 nm}}{\pi}a \tag{4}$$

and the chiral angle (θ), between 0 and $\pi/6$ rad, was described by Dresselhaus et al. (1995) by

$$\sin\theta = \frac{\sqrt{3}m}{2\sqrt{n^2 + m^2 + nm}} \qquad \cos\theta = \frac{2n + m}{2\sqrt{n^2 + m^2 + nm}} \tag{5}$$

Figure 1 illustrates the chiral angle and vector, respectively. Meanwhile, in figure 2 the three main SWNT configurations, i.e. armchair, zigzag and chiral, are described.

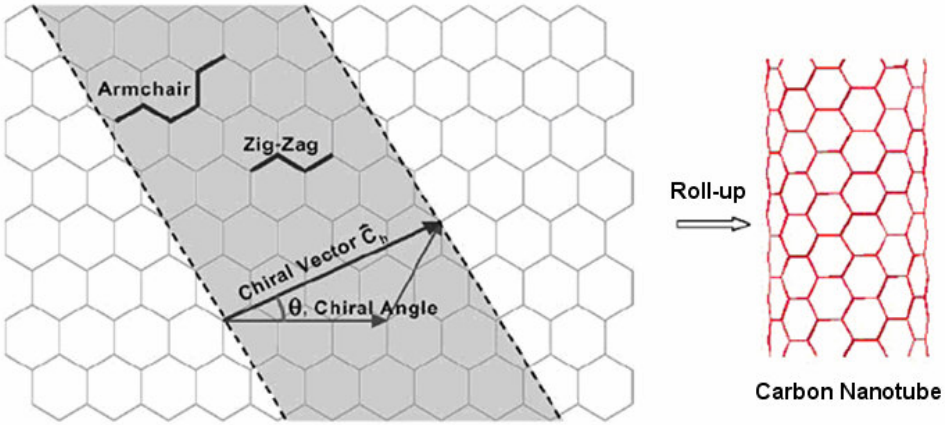

Figure 1. Chiral angle and vector representation. (Li and Chou, 2003)

In the molecular structural mechanics approach, a single-walled carbon nanotube is simulated as a space frame structure, with the covalent bonds and carbon atoms as connecting beams and joint nodes, respectively. If the beam elements simulating the covalent bonds are assumed to be of round section, then only three stiffness parameters, i.e., the tensile resistance *EA*, the flexural rigidity *EI* and the torsion stiffness *GJ*, need to be defined for deformation analysis. Li and Chou (2003), based on the energy equivalence between local potential energies in computational chemistry and elemental strain energies in structural mechanics, established a direct relationship between the structural mechanics parameters and the molecular mechanics force field constants. Such parameters are mathematically represented by:

$$\frac{EA}{L} = k_r \qquad \frac{EI}{L} = k_\theta \qquad \frac{GJ}{L} = k_\tau \tag{6}$$

where L denotes the bond length, and k_r , k_θ and k_τ are the force field constants in molecular mechanics. By assuming a circular beam cross section with diameter d, and setting A $=\pi d^2/4$, I$= \pi d^4/64$ and J$= \pi d^4/32$, Tserpes and Papanikos (2005) obtained the following expressions:

$$d = 4\sqrt{\frac{k_\theta}{k_r}} \qquad E = \frac{k_r^2 L}{4\pi k_\theta} \qquad G = \frac{k_r^2 k_\tau L}{8\pi k_\theta^2} \tag{7}$$

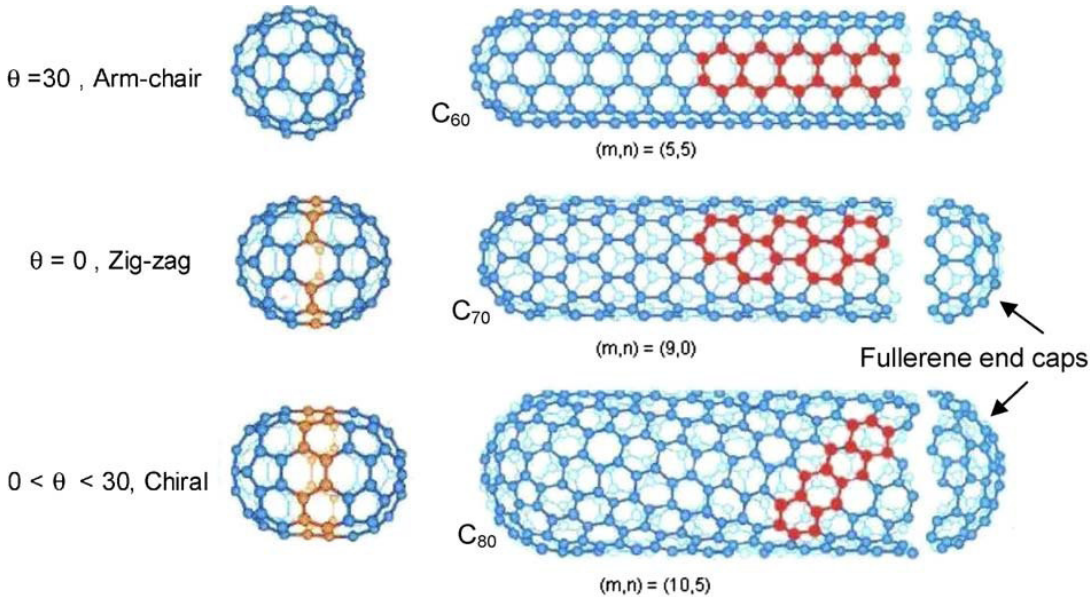

Figure 2. SWNT configurations and their respective caps (Kalamkarov et al., 2006)

As an illustrative example, Figure 3 shows the equivalence of molecular mechanics and structural mechanics for covalent and non-covalent interactions between carbon atoms.

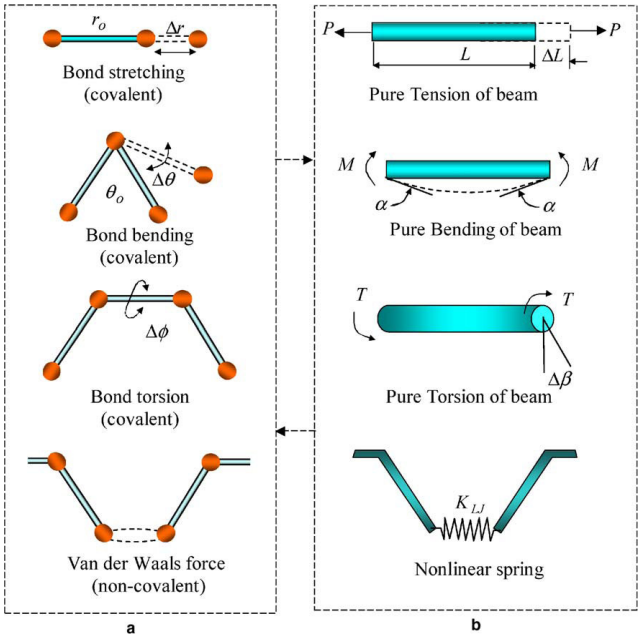

Figure 3. Equivalence between molecular and structural mechanics. (a) molecular mechanics; (b) structural mechanics (Kalamkarov et al., 2006)

Copyright © 2007 by ABCM

Li and Chou (2006) also proposed that for simulations of Van der Waals interactions between nested nanotube layers, a truss rod model was introduced by Li and Chou (2003). This model is based on the Lennard-Jones "6-12" potential and the van der Waals force between two atoms in the nearest neighboring tube layers can be written as

$$F(r) = 24\frac{\varepsilon}{\sigma}\left[2\left(\frac{\sigma}{r}\right)^{13} - \left(\frac{\sigma}{r}\right)^{7}\right] \tag{8}$$

where, r is the interatomic distance, ε and σ are the Lennard-Jones parameters. According to Li and Chou (2006), the activation of a truss rod is determined by the distance between the two atoms in the neighboring tube layers. If the distance is less than 2.5σ, a truss rod is assumed to be activated.

3. NUMERICAL SIMULATIONS AND ANALYSIS

The carbon-carbon bonds are simulated by a beam element with six degrees-of-freedom (DOF), i.e. three translations and three rotations, and length of 0.1421 nm as suggested by Tserpes and Papanikos (2005). To be able to generate each group of SWNT, i.e. armchair, zigzag and chiral a macro subroutine was developed and implemented into a commercial finite element commercial code named ANSYS V.10. In the present model, the k_r , k_θ and k_τ constants are from Li and Chou (2003), and their values are $6.52\text{x}10^{-7}$ N nm rad^{-1}, $8.76\text{x}10^{-10}$ N nm rad^{-2} and $2.78\text{x}10^{-10}$ N nm rad^{-2}, respectively. Figure 4 shows not only the model mesh for each SWNT group, but it also indicates the boundary conditions. The boundary conditions impositions are similar to load cases I and II described to Odegard et al. (2002). First, sub marginal nodes on one side of the generated nanotube were completely constrained, and them a prescribed displacement on axial direction was imposed on the nodes on the other side of the SWNT. Note that varying boundary conditions from imposing restrictions on axial directions only to constraining all DOFs do not have significant effect on reaction forces or nanotube deformation for the range of lengths used.

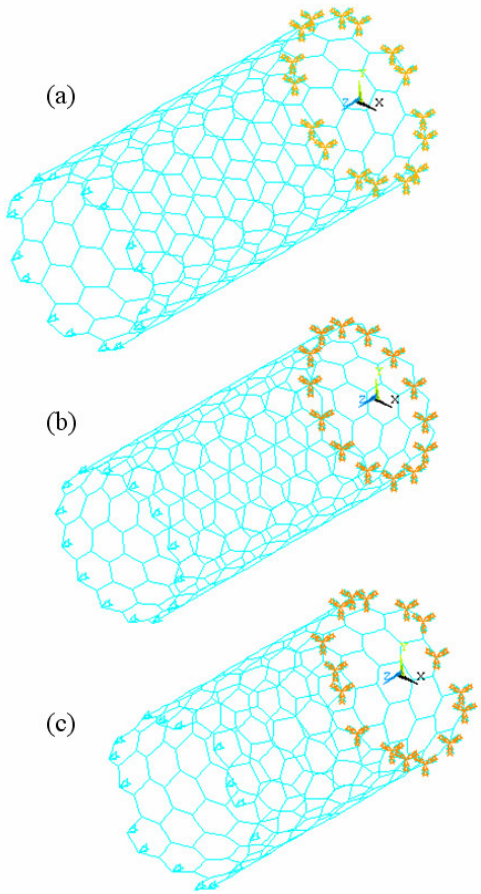

Figure 4. SWNT mesh and imposed boundary conditions. (a) (8,8) Armchair, (b) (14,0) zigzag, (c) (11,5) Chiral

The nanotubes generated varied from 112 atoms and 162 C-C bonds for the (4,2) chiral configuration to 623 atoms and 908 C-C bonds for the (17,9) chiral configuration. Table 1 shows the size of the Finite Element models for the nanotubes simulated, note that the number of nodes is corresponds to the number of atoms and the number of beam elements corresponds to the number of C-C bonds.

Table 1. Size of the Finite Element models

Configuration	Chirality (n,m)	Number of unit cells	Total length [nm]	Number of Nodes	Number of Beams
Armchair	(3,3)	10	2.3382	120	174
	(5,5)	10	2.3382	200	290
	(8,8)	10	2.3382	320	464
	(11,11)	10	2.3382	440	638
	(13,13)	10	2.3382	520	754
Zigzag	(5,0)	6	2.4157	120	175
	(9,0)	6	2.4157	216	315
	(14,0)	6	2.4157	336	490
	(19,0)	6	2.4157	456	665
	(23,0)	6	2.4157	552	805
Chiral	(4,2)	2	2.1854	112	162
	(6,4)	1	1.8130	152	218
	(11,5)	1	2.0123	268	386
	(14,8)	1	2.7255	496	722
	(17,9)	0.3	2.8986	623	908

Researchers such as Yakobson et al. (1996), Lu (1997), Hernandez at al. (1998), Odegard et al. (2002), Li and Chou (2003), Pantano and Parks (2004) agree that SWNT wall thickness has direct effect on stiffness. Therefore, to be able to exam how accurate the model's predictions are a series of simulations were performed considering these author's wall thickness and the results compared against their data. The three groups of SWNT are investigated, each one represented for a specific case, i.e. armchair (8,8), zigzag (14,0) and chiral (11,5). In Table 2 the results are summarized, while Figure 5 is the graphical representation of such data for the armchair (8,8) configuration.

Table 2: The wall thickness effect on stiffness

Investigators	Method Used	Young's Modulus [TPa]	Wall thickness [nm]	Present Work – Young's Modulus [TPa]		
				Armchair (8,8)	Zigzag (14,0)	Chiral (5,11)
Yakobson et al.	Molecular Dynamics	5.5	0.066	5.282	5.298	4.962
Pantano et al.	Continuum Shell Modeling	4.84	0.075	4.648	4.662	4.367
Li and Chou	Stiffness Matrix	1.01	0.34	1.025	1.028	0.963
Lu	Molecular Dynamics	0.974	0.34	1.025	1.028	0.963
Hernandez et al.	Tight binding MD	1.24	0.34	1.025	1.028	0.963
Odegard et al.	Equivalent-continuum modeling	-(1)	0.69	0.505	0.507	0.475
Tserpes and Papanikos	Finite Element Method	-(1)	0.147	2.377	2.385	2.423
Present Work	Finite Element Method	-(1)	0.1466	2.378	2.385	2.234

(1): these authors did not propose a single value for the Young's Modulus

The main difference on the results of the present work from the results from Tserpes and Papanikos are those for the chiral configuration. The difference may be caused by the nanotube length used. In the present work, as only unit cells of nanotube were used, the length of the SWNT's was taken as the distance between two homologous nodes at the unit cell in the two ends of the nanotube. This is very intuitive for the Armchair and Zigzag nanotubes, but, as the sub marginal nodes for the Chiral nanotube do not lie in the same sectional plane, the value of the actual length of nanotube becomes a hard task if unit cells are not used. The correct value is important when the calculation is done with a small length of SWNT's and to overcome this problem the use of a long nanotube would have the effect of the length diminished on the calculation of Young's modulus.

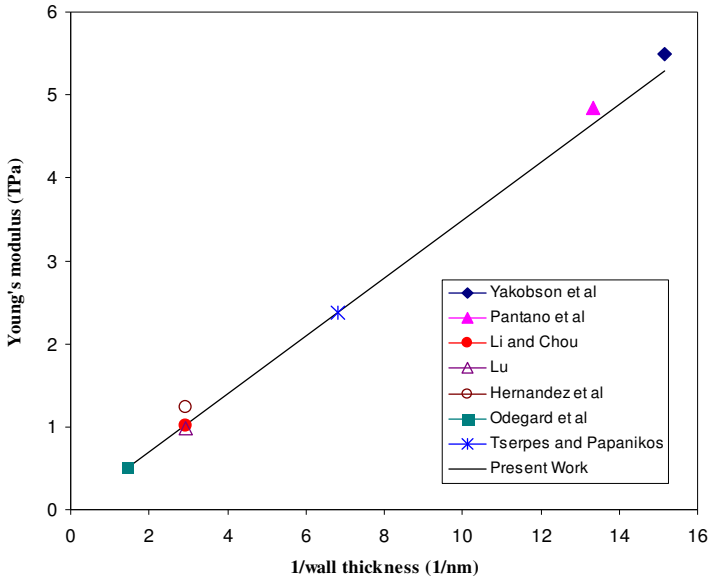

Figure 5. Comparison between the present model and various authors for the armchair (8,8) configuration

From Table 2 and Figure 5, it is clear that wall thickness has direct effect on stiffness. Larger walls lead to smaller Young's modulus. Such hypothesis can be corroborated by Odergard et al. (2002) whom, based on equivalent-continuum model, stated that Young's modulus is inversely proportional to SWNT cross sectional area. Furthermore, Li and Chou (2006) attributed the variation among the three configurations to small differences on radius. Tserpes and Papanikos (2005), however, also called the attention to the chirality's effect. According to them, the diameter effect is more evident on armchair and zigzag configurations, while the chiral form is less affected. With increasing tube diameter, the Young's modulus of SWNTs increases but not with the same trend for all SWNTs. Such event is observed in Figure 6. This phenomenon was explained by Li and Chou (2003) as the nanotube curvature effect. The smaller the nanotube diameter the higher the curvature resulting in large distortion of the carbon–carbon (C–C) bonds and therefore, in large elongation (Δh) of the nanotube. As diameter increases, the effect of curvature diminishes and the Young's modulus of SWNTs approaches that of graphene sheet (1.1 TPa) when considering 0.34nm as the wall thickness, for which no effect of curvature is present. The large discrepancy between the model prediction and the result presented by Hernandez et al. (1998) can be attributed to experimental inaccuracy during the measurements. Note that for the 0.34 nm the results are around 1.0 TPa.

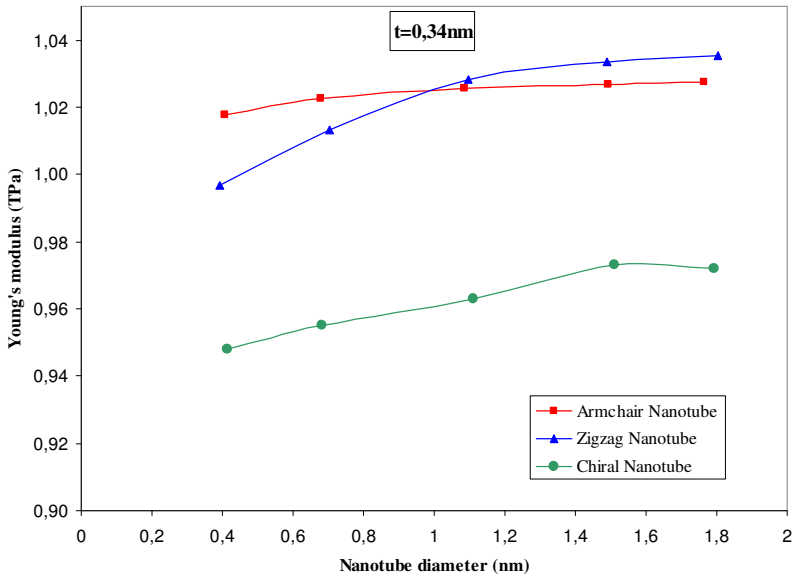

Figure 6. Variation of the Young's Modulus with nanotube diameter for armchair, zigzag and chiral configurations.

The concept of representative element volume described by Tamma and Avila (1999) was employed to isolate a unit cell and analyze the stress distribution over it. For a carbon nanotube, the unit cell is represented by a set of C-C bonds rings. The number of sets is defined by the SWNT configuration. The largest normal stress for the armchair configuration, showed in Fig. 7a, is located into bond angle variation region. Meanwhile, the zigzag format, showed in Fig. 7b, has the largest normal stress distribution on dihedral angle torsion region. These finds agree with analytical predictions made by Lu and Zhang (2006) where pointed these locations as the ones with highest probability of failure. As expected the stress distribution for the chiral configuration, represented in Fig. 8, is much more complex, where to largest normal stress is found in different points along the SWNT length.

As it was observed wall thickness does have effect on SWNT stiffness. Moreover, the SWNT radius influences the stiffness due to the curvature effect. Smaller radius implies larger curvature and consequently higher elongations and lower Young's Modulus. When failure mechanism is analyzed, the normal stress distribution directs us to locus of higher probability of failure. Those regions are the bond angle variation for the armchair configuration, the dihedral angle torsion region for the zigzag case, while the chiral configuration showed different regions of failure probability. Figures 9-11 show the deformed view for each case studied. Notice that for chiral case, the final deformed shape is distinct from the two others. It is a clear indication of a more complex stress/strain distribution.

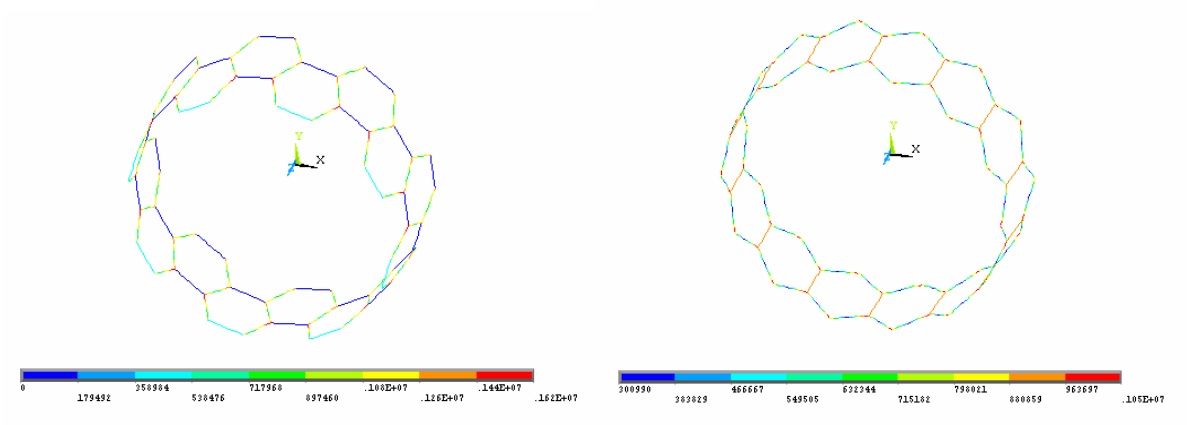

Figure 7. Normal stress distribution on armchair and zigzag SWNT unit cell respectively.

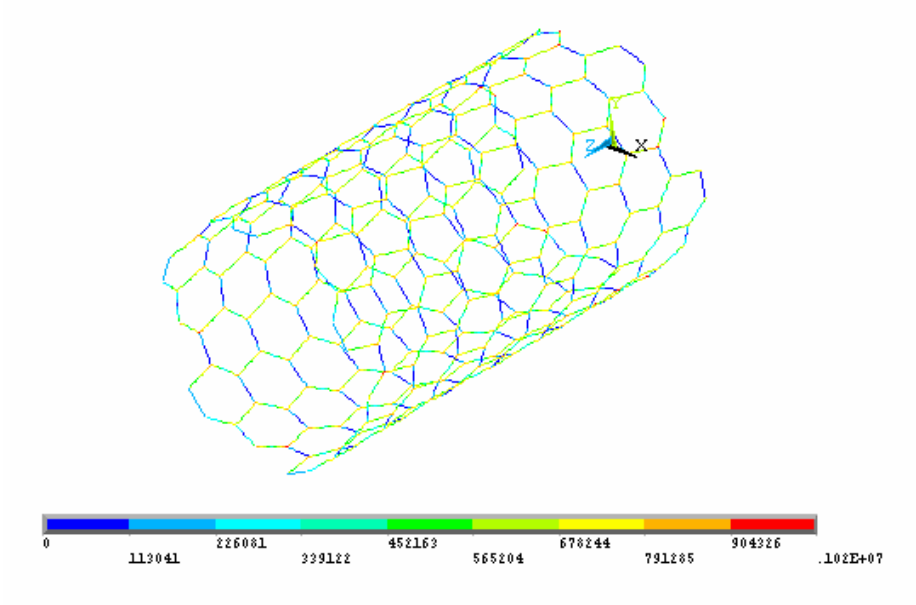

Figure 8. Normal stress distribution on chiral SWNT unit cell

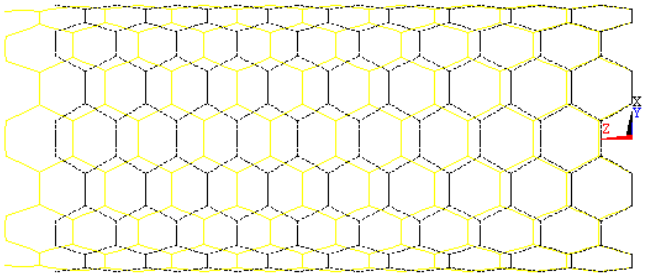

Figure 9. Deformed shape on a (8,8) armchair SWNT

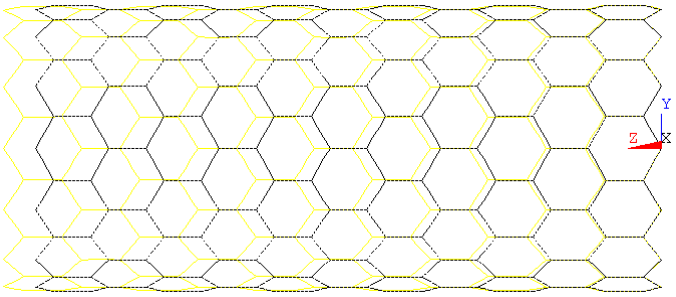

Figure 10. Deformed shape on a (14,0) zigzag SWNT

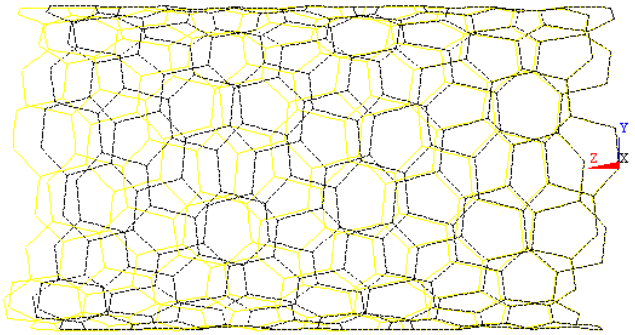

Figure 11. Deformed shape on a (11,5) chiral SWNT

4. CONCLUSIONS

A molecular mechanics model of armchair, zigzag and chiral single-walled carbon nanotubes has been implemented. The advantages of such approach are its easy implementation and considerably lower computational efforts when compared against other numerical techniques, e.g. molecular mechanics. The molecular structural mechanics approach was employed to exam the effect of wall thickness, diameter and chirality's effect on SWNT stiffness. The results suggested that stiffness (Young's modulus) is inversely proportional to wall thickness. Moreover, the curvature effect due to SWNT radius has also effect on stiffness. Smaller radius leads to larger curvatures and elongations. Meanwhile, on SWNT with large radius the curvature effect is negligible and Young's modulus is about the same as the graphene sheet (≈ 1.0 TPa). The SWNT configuration less affected by the radius/curvature variations seems to be with chiral one due to its complex geometry. The SWNT unit cell stress distributions also revealed critical regions where the failure is most likely to occur. For armchair case, it seems to be the bond angle variation region, while for the zigzag case the dihedral angle torsion region is the critical one. The chiral case presents a more complex distribution. The molecular structural mechanics approach is an effective atomistic modeling technique for simulating carbon nanotubes. Finally, this approach seems to be a powerful tool for modeling nanocomposites with accuracy.

5. ACKNOWLEDGEMENTS

The authors would like to acknowledge the financial support provided by the Brazilian Research Council (CNPq) grants 550067/2005-1 and 300826/2005-2 and the Institute of Nanotechnology (MCT/CNPq). Additional financial support, travel grants, provided by the Minas Gerais State Research Foundation (FAPEMIG) is also accredited.

6. REFERENCES

Dresselhaus MS, Dresslhaus G, Saito R, 1995, "Physics of carbon nanotubes", Carbon, Vol. 33, No. 7, pp. 883-891.

Hernandez E, Goze C, Bernier P, Rubio A, 1998, "Elastic properties of C and $B_xC_yN_z$ composite nanotubes", Physical Review Letters, Vol. 80, No. 20, pp. 4502–4505.

Huang M-Y, Chen H-b, Lu J-N, Zhang P-Q, 2006, "A modified molecular structural mechanics method for analysis of carbon nanotubes", Chinese Journal of Chemical Physics, Vol. 19, No. 4, pp. 286-290.

Kalamkarov AL, Georgiades AV, Rokkam SK, Veedu VP, Ghasemi-Nejhad MN, 2006, "Analytical and numerical techniques to predict carbon nanotubes properties", International Journal of Solids and Structures, Vol. 43, No. 20, pp. 6832-6854.

Koloczek J, Kwon Y-K, Burian A, 2001, "Characterization of spatial correlations in carbon nanotubes-modeling studies", Journal of Alloys and Compounds, Vol. 328, No. 2, pp. 222-225.

Krishnan A, Dujardin E, Ebbesen TW, Yianilos PN, Treacy MMJ, 1998, "Young's modulus of single-walled nanotubes", Physics Review B, Vol. 58, No. 20, pp. 4013–4019.

Li C, Chou TW, 2003, "A structural mechanics approach for the analysis of carbon nanotubes", International Journal of Solids and Structures, Vol.40, No.10, pp. 2487–2499.

Li C, Chou T-W, 2006, "Modeling Carbon Nanotubes in their Composites", In: Nanomechanics of Materials and Structures, T.J. Chuang et al. (editors), Springer, Amsterdam, pp. 55-65.

Liu WK, Park HS, Qian D, Karpov EG, Kadowaki H, Wagner GJ, 2006, "Bridging scale methods for nanomechanics and materials", Computational Methods and Applied Mechanics in Engineering, Vol. 195, No. 12, pp. 1407–1421.

Lourie O, Wagner HD, 1998, "Evaluation of Young's modulus of carbon nanotubes by micro-Raman spectroscopy", Journal of Materials Research, Vol. 13, No. 20, pp. 2418–22.

Lu JP, 1997, "Elastic properties of carbon nanotubes and nanoropes", Physical Review Letters, Vol. 79, No. 7, pp. 1297–300.

Lu J, Zhang L, 2006, "Analysis of localized failure of single-wall carbon nanotubes", Computational Materials Science, Vol. 35, No. 3, pp. 432-441.

Meo M, Rossi M, 2006, "Prediction of Young's modulus of single wall carbon nanotubes by molecular-mechanics based finite element method", Composites Science and Technology, Vol. 66, No. 10, pp. 1597-1605.

Natsuki T, Tantrakarn K, Endo M, 2004, "Effects of carbon nanotube structures on mechanical properties", Applied Physics A: Materials Science and Processing, Vol. 79, No. 1, pp. 117-124.

Odegard GM, Gates TS, Nicholson LM, Wise KE, 2002, "Equivalent continuum modeling of nano-structured materials", Composites Science and Technology, Vol. 62, No. 10, pp. 1869–1880.

Pantano A, Parks DM, Boyce MC, 2004, "Mechanics of deformation of single- and multi-wall carbon nanotubes", Journal of the Mechanics and Physics of Solids, Vol. 52, No. 6, pp. 789-821.

Saito R, Dresselhaus G, Dresselhaus MS, 2005, "Physical Properties of Carbon Nanotubes", Imperial College Press, London, pp. 35-94.

Sun X, Zhao W, 2005, "Prediction of stiffness and strength of single-walled carbon nanotubes by molecular-mechanics based finite element approach", Materials Science and Engineering A, Vol. 390, No. 3, pp. 366-371.

Tamma KK, Avila AF, 1999, "An Integrated Micro/Macro Modeling and Computational Methodology for High Temperature Composites", In Thermal Stress V, edited by Richard B. Hetnarski, Honeoeye Falls: Lastran Corporation, Vol. 05, pp. 143-256.

Tserpes KI, Papanikos P, 2005, "Finite Element modeling of single-walled carbon nanotubes", Composite: Part B, Vol. 36, No. 4, pp. 468-477.

Wang Y, Sun C, Sun X, Hinkley J, Odegard GM, Gates TS, 2003, "2-D nano-scale finite element analysis of a polymer field", Composites Science and Technology, Vol.63, No.10, pp. 1581–1590.

Xiao JR, Gama BA, Gillespie Jr. JW, 2005, "An analytical molecular structural mechanics model for the mechanical properties of carbon nanotubes", International Journal of Solids and Structures, Vol. 42, No. 24, pp. 3075–3092.

Yakobson BI, Brabec CJ, Bernholc J, 1996, "Nanomechanics of carbon tubes: instabilities beyond linear range", Physical Review Letters, Vol. 76, No. 20, pp. 2511–2514.

Yu MF, Lourie O, Dyer MJ, Moloni K, Kelly TF, Ruoff RS, 2000, "Strength and breaking mechanics of multiwalled carbon nanotubes under tensile load", Science Vol. 287, No. 6, pp. 637–640.

Zienkiewicz OC, Taylor RL, 1989, "The Finite Element Method", McGraw-Hill, New York.

7. RESPONSIBILITY NOTICE

The authors are the only responsible for the printed material included in this paper.